

4-1-2008

Analysis and Suppression of Base Separation in the Casting of a Cylindrical Ingot

Ravi Annapragada
asravi@purdue.edu

Dawei Sun

S V. Garimella
Purdue Univ, sureshg@purdue.edu

Follow this and additional works at: <http://docs.lib.purdue.edu/coolingpubs>

Annapragada, Ravi; Sun, Dawei; and Garimella, S V., "Analysis and Suppression of Base Separation in the Casting of a Cylindrical Ingot" (2008). *CTRC Research Publications*. Paper 100.
<http://docs.lib.purdue.edu/coolingpubs/100>

This document has been made available through Purdue e-Pubs, a service of the Purdue University Libraries. Please contact epubs@purdue.edu for additional information.

This article was downloaded by:[Purdue University]
On: 20 February 2008
Access Details: [subscription number 768489986]
Publisher: Taylor & Francis
Informa Ltd Registered in England and Wales Registered Number: 1072954
Registered office: Mortimer House, 37-41 Mortimer Street, London W1T 3JH, UK



Heat Transfer Engineering

Publication details, including instructions for authors and subscription information:
<http://www.informaworld.com/smpp/title~content=t713723051>

Analysis and Suppression of Base Separation in the Casting of a Cylindrical Ingot

S. Ravi Annapragada ^a; Dawei Sun ^a; Suresh V. Garimella ^a

^a School of Mechanical Engineering, Purdue University, West Lafayette, Indiana, USA

Online Publication Date: 01 April 2008

To cite this Article: Annapragada, S. Ravi, Sun, Dawei and Garimella, Suresh V. (2008) 'Analysis and Suppression of Base Separation in the Casting of a Cylindrical Ingot', Heat Transfer Engineering, 29:4, 385 - 394

To link to this article: DOI: 10.1080/01457630701825671

URL: <http://dx.doi.org/10.1080/01457630701825671>

PLEASE SCROLL DOWN FOR ARTICLE

Full terms and conditions of use: <http://www.informaworld.com/terms-and-conditions-of-access.pdf>

This article maybe used for research, teaching and private study purposes. Any substantial or systematic reproduction, re-distribution, re-selling, loan or sub-licensing, systematic supply or distribution in any form to anyone is expressly forbidden.

The publisher does not give any warranty express or implied or make any representation that the contents will be complete or accurate or up to date. The accuracy of any instructions, formulae and drug doses should be independently verified with primary sources. The publisher shall not be liable for any loss, actions, claims, proceedings, demand or costs or damages whatsoever or howsoever caused arising directly or indirectly in connection with or arising out of the use of this material.

Analysis and Suppression of Base Separation in the Casting of a Cylindrical Ingot

S. RAVI ANNAPRAGADA, DAWEI SUN, and SURESH V. GARIMELLA

School of Mechanical Engineering, Purdue University, West Lafayette, Indiana, USA

This paper presents a comprehensive numerical investigation of the influence of cooling conditions on base separation, void formation, and thermally induced stresses during the solidification of a high Prandtl number energetic melt in a cylindrical enclosure. Numerical models have been developed to simulate the heat and mass transfer processes in melt casting as well as analyze the base separation and thermal stresses induced during solidification. Two models are dynamically coupled, and the numerical predictions are validated against experiments. Based on the numerical analysis, modified cooling conditions are suggested that are shown to reduce base separation.

INTRODUCTION

Casting is an established and widely used process for manufacturing complex shapes without the necessity of applying large forces. It is especially useful in processing energetic materials that cannot tolerate high forces. The ambient cooling conditions play an important role in determining the quality of the final cast product. One measure of quality is the nearness of the product to the final shape desired with little or no residual stresses. An example of deviation from the desired shape is base separation [1]. Well-designed cooling conditions could help avoid such deleterious effects.

In casting processes, the heat transfer, fluid flow, and phase change processes and induced stresses are strongly coupled. The effects of natural convection in the melt induced by solidification are relatively well understood. Extensive analytical, experimental, and numerical efforts have been reported on this topic [1–6].

Thermal stresses induced during the casting process are, in general, less well understood. Analytical solutions have been suggested under simpler conditions and geometries such as high-pressure die casting [7]. It is also challenging to experimentally visualize thermal stresses. Interesting approaches such as the use of x-ray diffraction [8] and neutron diffraction [9] have been suggested. However, these approaches require high-intensity emit-

ters and can be prohibitively expensive. Moreover, transient development of the three-dimensional stress field is very difficult to map. Numerical simulation of thermal stresses also poses several challenges. The stress analysis must consider dynamic coupling between solidification heat transfer and the resulting stresses induced in order to predict the developing gap between mold and cast product. The governing equations for thermal transport and stress should be coupled to model the transient development of thermal stresses.

Finite element methods (FEM) have been widely used to numerically simulate casting problems. Thomas [10] reviewed in detail the various FEM thermal stress models and discussed difficulties in practical implementation. Contact conductance between the casting and the mold was modeled by Fackeldey et al. [11] as a simple function of pressure. But the separation of the casting from the mold, which has a detrimental effect on heat transfer, was neglected. Several models have been proposed to address this separation. Seetharamu et al. [12] considered the loss of contact between the mold and the cast, and modeled the heat transfer as being across an air gap. Isaac et al. [13] predicted the size and distribution of the separation and modeled it as gap conductance.

Accurate materials characterization is also important for modeling thermal stresses, as, in general, materials change from viscoelastic/viscoplastic in the liquid phase to elastic-plastic in the solid phase [14]. However, no generic constitutive relationships exist (other than for certain metals such as steel and aluminum), and experimental or empirical data [1, 15, 16] have to be relied upon.

Address correspondence to Dr. Suresh V. Garimella, School of Mechanical Engineering, 585 Purdue Mall, Purdue University, West Lafayette, Indiana 47907-2088, USA. E-mail: sureshg@purdue.edu

The modeling of solidification and tracking of the solid front are also complicated by the steep jump in material properties across the front. In some stress analyses, simplified analytical solutions have been used to track the solid front location and stress development [17]. Stresses induced during the continuous casting of slabs were solved with a heat generation term in the steady-state heat conduction equation used to account for phase change [18]. Recently, a thermomechanical model for the continuous casting of steel was proposed by Li and Thomas [19]. Constitutive equations were formulated, and the finite element method was used in the computations. The effect of melt convection has generally been neglected in these studies.

Integrated models incorporating fluid flow and solidification into residual stress analyses have also been attempted. In such cases, the temperature distribution was calculated using finite volume [20] or finite difference [21] methods, while the stress field was handled with finite difference [20] or FEM [21] approaches. In one study [22], both phase change with melt convection and stresses were analyzed in the same solver.

The thermal stress distribution has been shown to be closely related to cold cracks, hot tears, and butt curl in aluminum casting [1, 15]. Actual deformation from the desired shape in the form of butt curl was investigated by Barral and Quintela [1]. Hannart et al. [16] investigated the butt curl phenomenon in direct chill casting of aluminum slabs by assuming the metal to be elastic-plastic with strain rate-dependent behavior. A butt curl mechanism was proposed for sheet ingots (with a width to thickness ratio of 3) based on bending due to differential expansion [15]. Using finite volume and finite element methods, a preliminary study of both solidification heat transfer and residual stress during the casting of high Prandtl number fluids was carried out by Sun et al. [4, 23]. The effect of changing the cooling conditions on the resulting stresses was investigated. The stress analysis was decoupled from the flow and heat transfer analysis.

The objective of the present work is to develop an integrated finite volume-finite element computational model to analyze phase change heat transfer with melt convection and the development of the stress field during the casting of a high Prandtl number fluid in a cylinder. User-defined routines are developed to perform the computations with two commercial software packages (FLUENT [24] for the thermal analysis and ANSYS [25] for the stress analysis).

THE CASTING PROBLEM UNDER CONSIDERATION

A schematic diagram of the mold/riser assembly considered in this work is shown in Figure 1. The mold and riser are made of stainless steel (AISI 302) and aluminum (Alloy 7075-T6), respectively. A steam heater is placed on top of the riser, and the sidewalls are cooled by natural convection. More information about the experimental setup is available in Sun et al. [4, 23]. The test specimen is instrumented with 15 K-type thermocouples inside the casting. The black dots in Figure 1 show three of the 15

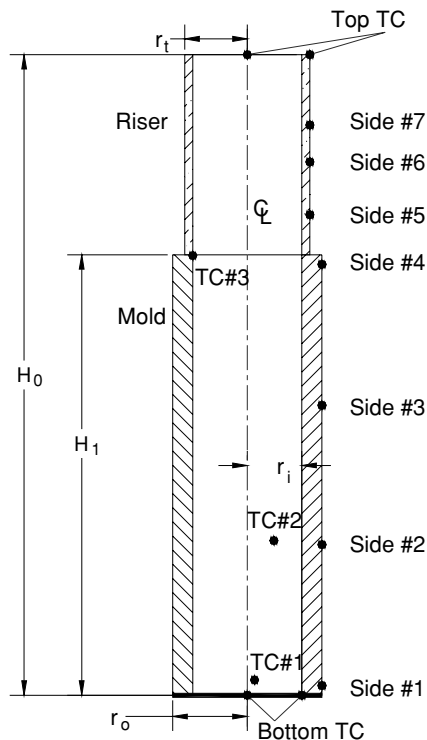


Figure 1 Schematic diagram of the cylindrical casting used in the experiment with thermocouple locations.

internal thermocouple locations, as well as those along the sidewall, top surface, and bottom surface. A high Prandtl number material, Picatinny Arsenal Explosive (PAX) material, composed of 83%wt cyclo-trimethylene-trinitramine (RDX) particles and 17%wt carnauba wax, is considered in this work. Only the wax undergoes solid/liquid phase change during casting. Effective thermophysical properties of this material are listed in Table 1. These effective properties can be evaluated numerically using the microstructural RVE models developed by Annapragada et al. [26]. The Young's modulus for this material is shown in Figure 2. The thermophysical properties for the mold and riser can be found in Table 2 [27, 28].

Melt at 360 K is poured into the mold and riser assembly shown in Figure 2. A steam heater is then placed on the top to maintain the riser at a higher temperature while the sides are exposed to natural convection by ambient air at 311 K, resulting in a natural convection coefficient of 6 W/m²K. The heaters are

Table 1 Thermophysical properties of the high Prandtl-number energetic material being cast

Density, ρ	1562 kg/m ³
Thermal conductivity, k_{eff}	0.428 W/(m·K)
Specific heat, c_p	1524 J/(kg·K)
Viscosity, μ	3.11 Pa·s
Melting temperature, T_m	355.65 K
Latent heat, ΔH	14.83 kJ/kg
Poisson ratio, ν	0.22
Liquid thermal expansion coefficient, β_l	1.11×10^{-4} 1/K
Solid thermal expansion coefficient, β_s	8.754×10^{-5} 1/K

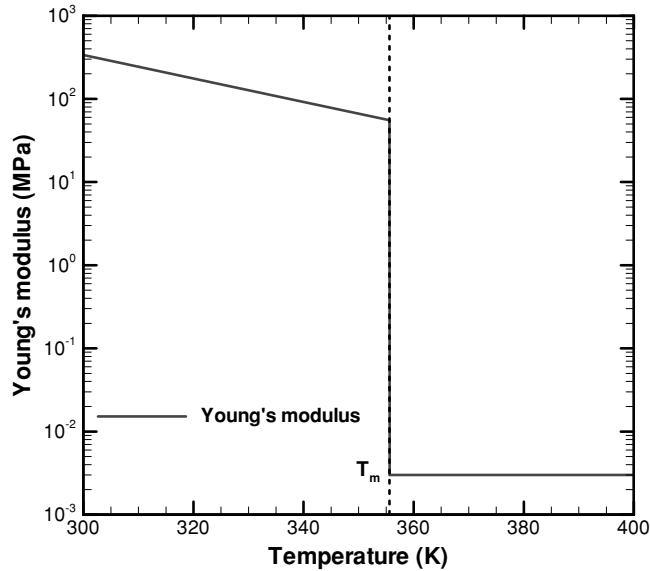


Figure 2 Temperature-dependent Young's modulus for the energetic material undergoing solidification.

switched off after 2.2 hours, and then the whole assembly is cooled by natural convection. The total solidification process takes about 2.5 hours.

Temperature boundary conditions imposed in the experiment are measured using seven thermocouples mounted on the outer wall and four thermocouples on the top and bottom surfaces to obtain transient vertical and circumferential temperature variation, as shown in Figure 3. (for clarity, only selected locations along the sidewall are included). The transient cooling conditions, with the sidewall being at a lower temperature than the bottom surface from the beginning of the casting process, would be expected to lead to complex contraction/shrinkage patterns in the casting.

COMPUTATIONAL MODEL

As the rheological behavior of the high-viscosity, particle-laden (greater than 80% solid fraction of particles) energetic material considered in this work is not fully understood, the fluid is assumed to be incompressible and Newtonian. Although the model can account for the temperature dependence of thermo-physical properties, the properties are assumed to remain constant over the range of temperatures investigated in this work.

Table 2 Thermophysical properties of the mold and riser

Thermophysical properties	Mold	Riser
Density, ρ (kg/m ³)	8030	2719
Thermal conductivity, k	16.27	202.4
Specific heat, c_p (J/(kg·K))	502.48	871
Young's modulus (Pa)	2.1×10^{11}	7.2×10^{10}
Poisson ratio	0.3	0.345
Thermal expansion coefficient, β (1/K)	1.24×10^{-5}	2.36×10^{-5}

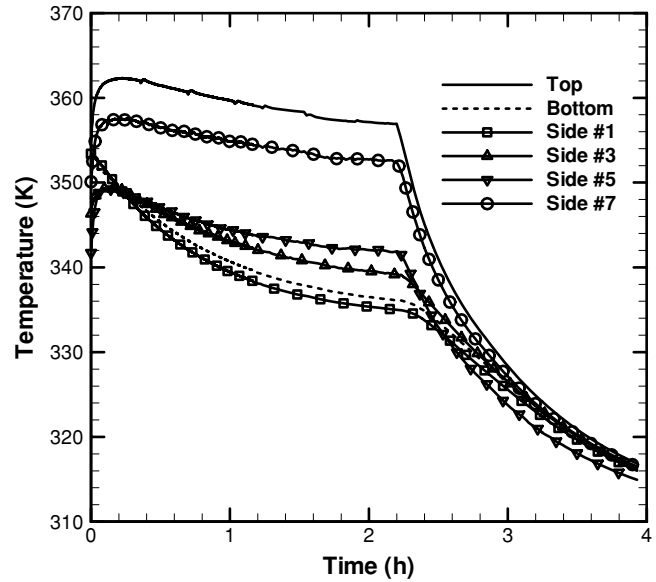


Figure 3 Temperature boundary conditions applied to the top, bottom, and side walls of the cylinder during the experiment.

The governing mass, momentum and energy equations are:

$$\frac{\partial \rho}{\partial t} + \nabla \cdot (\rho \vec{v}) = 0 \quad (1)$$

$$\left(\frac{\partial \rho u_i}{\partial t} + \frac{\partial \rho u_i u_j}{\partial x_j} \right) = -\frac{\partial p}{\partial x_i} + \frac{\partial}{\partial x_j} \left[\mu \left(\frac{\partial u_i}{\partial x_j} + \frac{\partial u_j}{\partial x_i} \right) \right] + \rho_\infty g_i \beta (T - T_\infty) + \frac{(1 - f_l)^2}{(f_l^3 + \epsilon)} A_{mush} u_i \quad (2)$$

$$\frac{\partial \rho h}{\partial t} + \frac{\partial}{\partial x_j} (\rho u_j h) = \frac{\partial}{\partial x_i} \left(k \frac{\partial T}{\partial x_i} \right) \quad (3)$$

where A_{mush} is the mushy zone constant, f_l the liquid fraction, $\epsilon = 0.001$ is used to prevent division by zero, and $h = c_p T + f_l \Delta H$ the specific enthalpy of the melt [24]. The above equations were solved using FLUENT with custom user-defined functions (UDFs) developed in this work. The enthalpy method [29] was employed to model solidification, and the SIMPLEC algorithm was used for pressure-velocity coupling. Second-order discretization schemes were used for both momentum and energy equations for improved accuracy, and the pressure staggered option (PRESTO!) was adopted for discretizing the pressure term. The volume change during solidification was ignored. In view of the very thin thermal boundary layer and low velocities observed in high Prandtl number materials, regions near the boundaries in the computational domain were very finely resolved.

The solidifying melt was modeled as a single material with temperature-dependent thermal expansion coefficient and Young's modulus, with all other properties remaining the same in both solid and liquid phases, as shown in Table 1. In the absence of detailed visco-elastic-plastic material properties, the material

was treated as an isotropic thermo-elastic material, defined by the following differential equation:

$$\frac{\partial}{\partial t} \left(\rho \frac{\partial \vec{w}}{\partial t} \right) = \nabla \cdot [\mu(\nabla \vec{w} + \nabla \vec{w}^T)] + \nabla (\lambda \nabla \cdot \vec{w} + (3\lambda + 2\mu) \beta_s T) - \left\{ \nabla \cdot \left[\frac{\sigma_{ij}^d \sigma_{kl}^d}{\bar{\sigma}^2} \left(\frac{9G^2}{H' + 3G} \right) \nabla \vec{w} \right] \right\} + \vec{b} \quad (4)$$

where

$$\lambda = \frac{\nu E}{(1 + \nu)(1 - 2\nu)}$$

This equation is solved in ANSYS [25]. It should be noted that no relative displacement is allowed between the metal and the melt boundaries, implying perfect contact at this interface.

Coupling Methodology

One-way coupling was implemented between FLUENT and ANSYS to solve for thermal stresses during the casting process. The coupling scheme is graphically illustrated in Figure 4.

Identical grids are used for both FLUENT and ANSYS (grid-independence is discussed later in this paper). The thermal field predicted by FLUENT is fed into ANSYS as a “body load” to all the elements. The temperature body load is maintained constant for the whole time interval while calculating stress and displacement. Within each time interval, the transient stress and displacement fields are solved in a quasi-transient fashion in which the stress and displacement fields prevailing at the previous time step are used as initial values for the following time interval. The temperature load remains constant while stress

and displacements fields are being solved. Deformation of the computational mesh due to stress-induced displacement is neglected in the current implementation, as is the resulting gap formation. The coupled model represents a convenient tool to model thermal stresses and displacement in the current casting problem.

RESULTS AND DISCUSSION

The coupled model is first benchmarked against results from the literature. It is then used to predict the stress and displacement fields in the casting of a high Prandtl number energetic material.

Coupled-Model Validation

The benchmark problem considered for validating the coupled model is the elastic-plastic stress development in an unconstrained solidifying plate [17], as shown in Figure 5. The Neumann problem for solidification is studied (i.e., the left wall of a semi-infinite plate initially maintained at its melting point T_m) is suddenly exposed to a temperature $T_w < T_m$ initiating solidification. Material properties and other related constants used in this validation are shown in Table 3 [19]. The yield stress of the material σ_0 is assumed to be a linear function of temperature, defined as:

$$\sigma_0(T) = \sigma_{0,W} \frac{T - T_m}{T_w - T_m} \quad (5)$$

where $\sigma_{0,W}$ is the yield stress at T_w .

The y-direction stress σ_{yy} is the significant stress component [17] in this problem. Temperature and σ_{yy} distributions along the x-direction can be solved analytically [17, 30]. The proposed coupled model is employed to solve this problem with a plane strain condition. It is evident from Eq. (5) that $\sigma_0 = 0$ at the melting temperature T_m ; however, to avoid numerical difficulties, a value of $\sigma_0 = 0.1$ MPa is used. Predictions from the model are compared to the analytical results for temperature and stress profiles at selected times in Figure 6; the agreement is seen to be quite satisfactory.

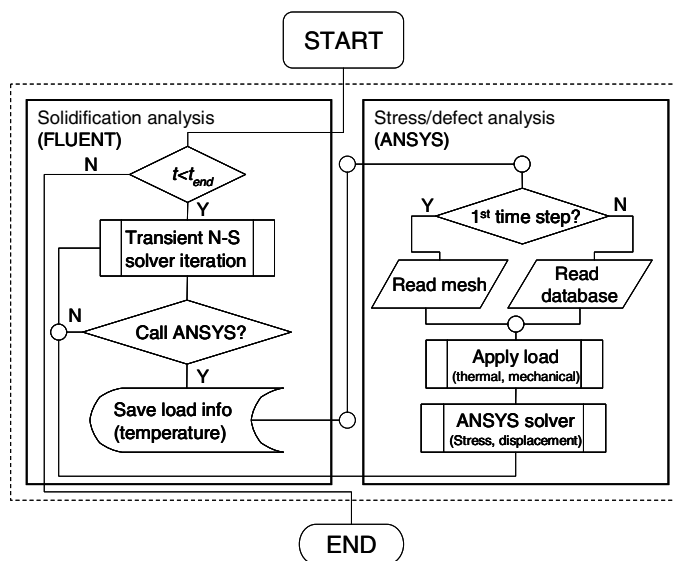


Figure 4 Flow chart for coupling solidification heat transfer and residual stress analysis.

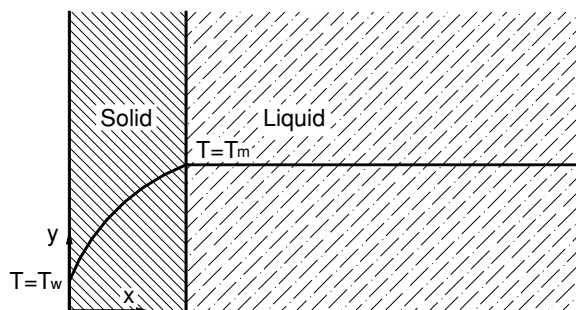


Figure 5 Physical problem considered for validating the current modeling approach [17].

Table 3 Thermophysical properties and other constants used in the validation exercise [19]

Density, ρ (kg/m ³)	7500
Thermal conductivity, k (W/m-K)	33
Specific heat, c_p (J/kg-K)	661
Elastic modulus of solid, E_s (GPa)	40
Elastic modulus of liquid, E_l (GPa)	14
Poisson's ratio, ν	0.3
Thermal expansion coefficient, β (1/K)	2×10^{-5}
Melting temperature, T_m (°C)	1494.4
Latent heat, ΔH (kJ/kg)	272.0
Wall temperature, T_w (°C)	1000
Yield stress at T_w , $\sigma_{0,w}$ (MPa)	20

Solidification in a Cylindrical Casting

The numerical model developed in this work is validated against experimental temperature measurements, and the comparisons at representative locations are shown in Figure 7. The

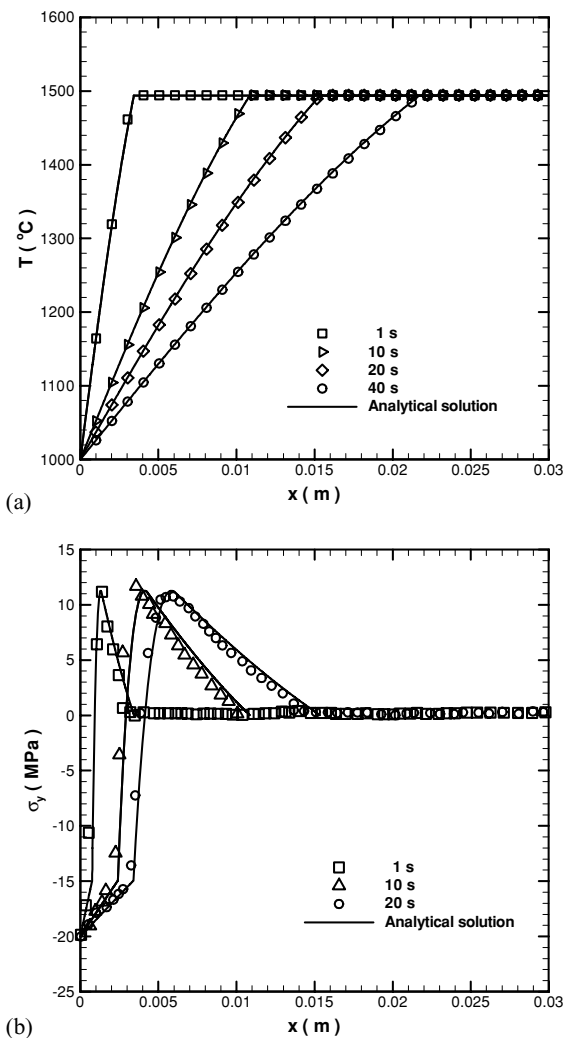


Figure 6 Comparison of (a) temperature, and (b) y-direction stresses σ_{yy} in the solidifying body predicted by the numerical model with analytical results.

Table 4 Meshes in the grid-independence study

	Coarse	Intermediate	Fine
Riser	20×2	40×4	80×8
Mold	40×4	80×8	160×16
Casting	60×20	80×40	160×80

good agreement in this figure is an improvement over earlier predictions [4, 23]. This is attributed to the more comprehensive experimental measurements obtained for this work, including temperature measurements during the first 10 minutes of the solidification process, after pouring. Data during this period are critical in setting the conditions for subsequent solidification. The minor deviations that can still be seen in the figure are in part due to the uncertainties in the thermophysical properties.

A grid-independent study was carried out in which three levels of successively refined meshes (see Table 4) were evaluated; results with these grids at two different times are shown in Table 5. The times are chosen as those at which convective effects are strong. The temperatures listed in the table are at the location ($r = 0.01$ m, $z = 0.05$ m). The moderate mesh in Table 4 was used for the results in this study, and deviations in Table 5 are calculated as

$$\varphi\%_i = \frac{|\varphi_i - \varphi_m|}{|\varphi_m|}$$

in which φ is the variable and $i = c$ or f represents coarse and fine mesh, respectively. From Table 5, it may be concluded that satisfactory grid-independence was achieved using the moderate mesh.

The transient development of the thermal and flow fields in the domain is shown in Figure 8(A–D). The solidification front develops from the side and bottom walls during the initial stages (see Figure 8A). Because the riser temperature is maintained above the melting temperature of 355.65 K by the heaters, no solid front emanates from the top surface of the melt until 2.2 hours into the process, at which time the heater above the riser is switched off. Initially, a long natural convection cell is

Table 5 Results obtained with different grids

Grid	f_l	$ u _{\max}$ (m/s)	ψ_{\max} (m ² /s)	T (K)
t = 600 s				
Coarse	0.402	1.824×10^{-4}	4.631×10^{-6}	353.02
% Deviation	3.60	6.63	2.62	0.90
Intermediate	0.388	1.954×10^{-4}	4.513×10^{-6}	356.23
Fine	0.386	1.964×10^{-4}	4.503×10^{-6}	356.48
% Deviation	0.51	0.50	0.23	0.07
t = 1200 s				
Coarse	0.2581	6.541×10^{-5}	4.126×10^{-5}	350.21
% Deviation	10.58	2.34	1.72	0.72
Intermediate	0.2334	6.698×10^{-5}	4.198×10^{-5}	352.74
Fine	0.2302	6.702×10^{-5}	4.204×10^{-5}	352.86
% Deviation	1.38	0.06	0.14	0.03

Deviations are with respect to the intermediate grid.

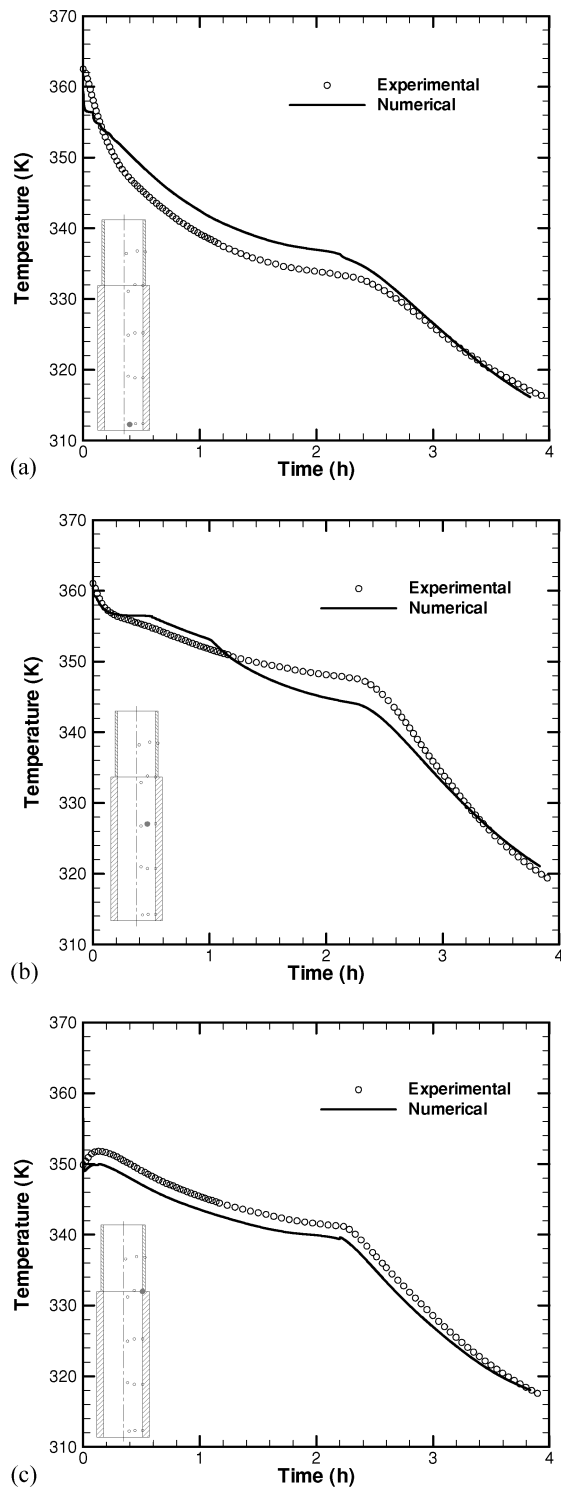


Figure 7 Comparison between measured temperature variations and numerical predictions at selected locations.

formed in the narrow channel ($H_0/D \approx 6$). This long convection cell breaks up as solidification progresses and the solid front from the side reaches the vertical axis, leaving behind pockets of melt in the lower region of the casting. One such liquid pocket can be seen in Figure 8B. This could be a potential site for void formation due to shrinkage.

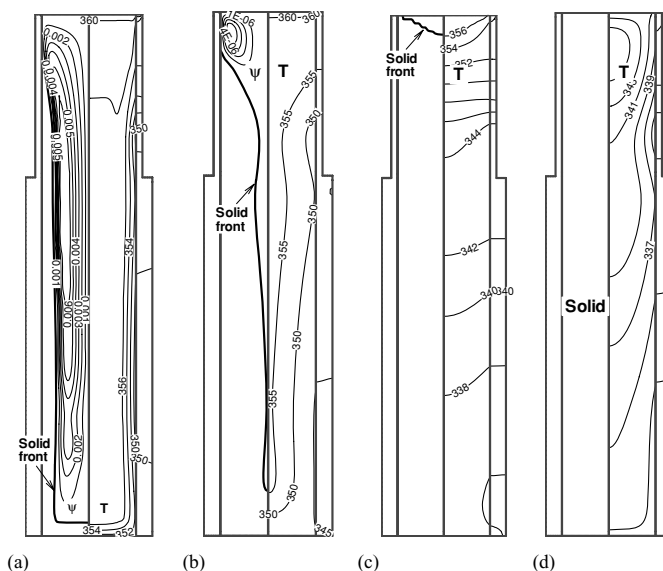


Figure 8 The development of stream function contours and isotherms during the course of the casting process: (a) $t = 5$ min, (b) $t = 30$ min, (c) $t = 2$ hours, and (d) $t = 2.5$ hours.

It may be noted that the maximum velocity induced by natural convection during the entire solidification process is 6.22×10^{-4} m/s ($Ra \approx 2200$), implying that natural convection effects are negligible under these conditions.

Once the heaters above the riser are switched off, the solid front develops from all sides, including the top due to the presence of cold environment. As shown in Figure 8D, the solidification process is completed in 2.25 hours. Additional discussion of the transient temperature and solid front development is available in [4, 23]. The temperature distribution at the end of the solidification process can lead to the induction of residual stresses and base separation, and this is the focus of the present work.

Displacement and Stress Fields

During the casting process, displacement fields and residual stresses are induced due to the combined effect of temperature distribution in the casting and the different thermal expansion coefficients between the steel metal mold ($\beta_{\text{steel}} = 1.24 \times 10^{-5}$) and the cast material ($\beta_{\text{cast}} = 8.754 \times 10^{-5}$). Figure 9 shows the experimentally measured temperature variation along one vertical line in the cast at various times near the beginning of casting process. The non-monotonic temperature profile shown in the figure results in the shrinkage being inward, toward the location of the lowest temperature. The vertical movement of the material near the sides is restricted by the steel mold, which has a smaller thermal expansion coefficient. Hence, the top and bottom surfaces of the material assume a concave surface due to greater unrestricted shrinkage near the axis as compared to the sides. This displacement of the bottom surface from the mold is termed base separation. Figure 10 conceptually illustrates the mechanism of base separation.

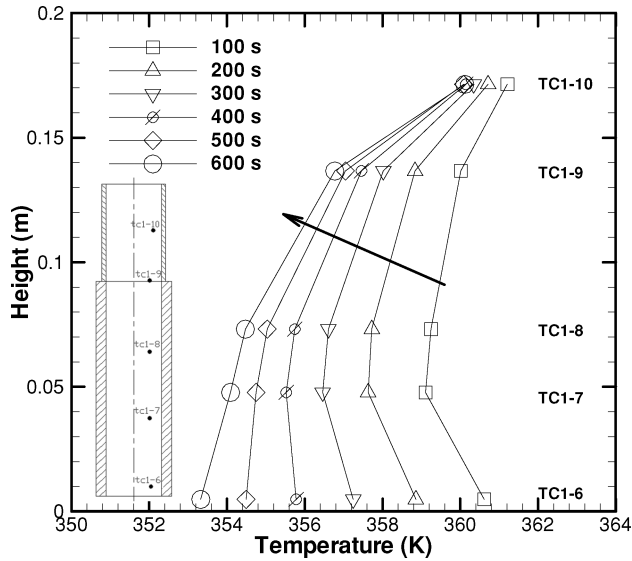


Figure 9 Temperature fields in the enclosure along a vertical plane at various times.

Base separation may be avoided by imposing boundary conditions that result in a monotonic temperature profile along the vertical direction, with the lowest temperature being at the bottom. Under these conditions, displacement of the solidified material would tend to be toward the bottom mold surface rather than away from it. The top open surface would still experience a concave shape due to shrinkage, but this is not of concern because the riser and the material inside is detached after casting and discarded.

To better illustrate the effects of experimental cooling conditions on residual stresses, the displacement and von Mises stress

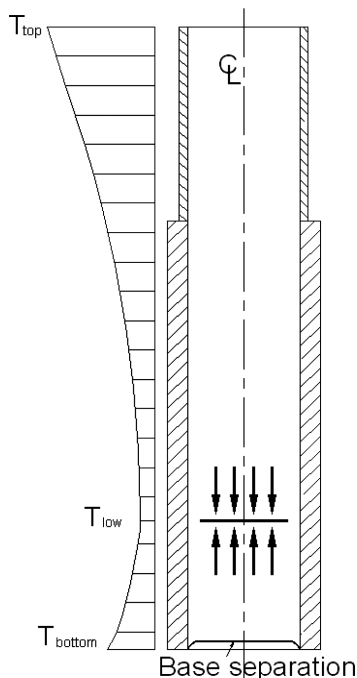


Figure 10 Conceptual illustration of the base separation mechanism.

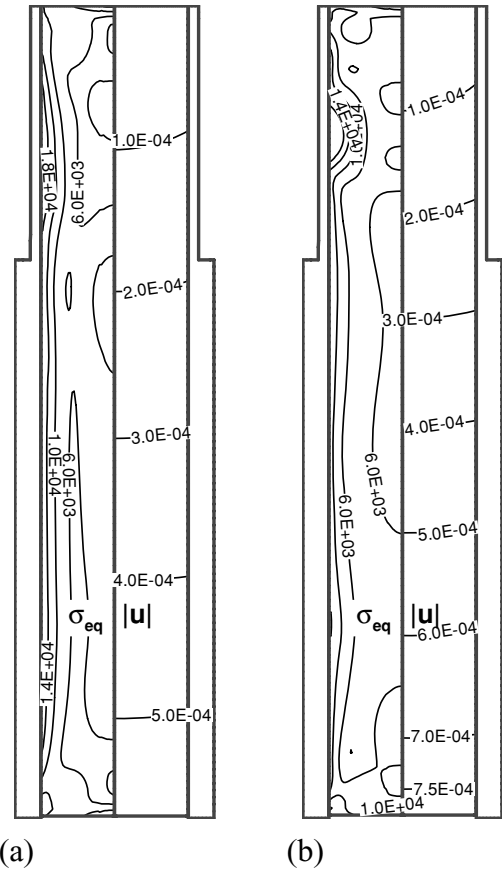


Figure 11 Stress (left) and vertical displacement (right) contours after solidification is completed at (a) 3 hrs and (b) 4 hrs into the casting process under the experimental conditions.

fields from the numerical simulations are shown in Figure 11; the vertical displacement is shown on the right in each panel and the von Mises stress on the left. Because the liquid is assumed to be stress-free in this work, the stress development in the solidified layer plays the determining role in the predicted displacement (i.e., separation). Because $\sigma \sim E\beta\Delta T$, a qualitative comparison of stresses in the mold and casting can be written as

$$\frac{\sigma_m}{\sigma_c} = \frac{(E\beta\Delta T)_m}{(E\beta\Delta T)_c} \approx \frac{(E\beta)_m}{(E\beta)_c} \approx 150 \quad (6)$$

Hence, much higher residual stresses were found in the mold and the riser compared with the cast. Also, because the mold and riser have lower expansion coefficients than the casting (see Tables 1 and 2), the differential contraction induces compressive stresses in the mold and tensile stresses in the solidified melt in all directions. This explains the high stresses observed along the outer surface of the casting. Due to the combined vertical and radial stresses, the stress contours reunite at various locations on the vertical axis.

The maximum base separation of 0.081 mm predicted from the coupled numerical model developed, which occurs at the lowest point on the vertical axis, is comparable to the experimentally measured value of 0.061 mm.

Reduction of Base Separation through Control of Boundary Conditions

An analysis of the results from the numerical model suggests modified boundary conditions that would lead to a more monotonic temperature profile in the vertical direction and, therefore, reduced base separation. The calculations shown thus far for the experimental cooling conditions (termed “original” case below) were repeated with modified conditions in which the top and bottom surfaces were assumed to be at 360 K and 343 K, respectively (instead of the experimentally measured conditions shown in Figure 11), for the first two hours, after which the top heaters are switched off and the top surface exposed to the ambient. The sides are exposed to the ambient at 311 K throughout the casting period, with a natural convection coefficient as before of 6 W/m²K. It is noted that only numerical results were obtained for the “modified” case, with no corresponding experiments.

Figure 12 shows a comparison of the displacements at the bottom surface of the specimens 3 hours into the casting process, obtained with the original and modified cooling conditions. A 25% reduction in the base separation is seen to result from the new cooling conditions. The new boundary conditions pin the displacement at the base such that all of the shrinkage is directed toward the base and allows reduced shrinkage. However, the natural air cooling along the side walls does not control the vertical temperature distribution to the extent desired, which contributes to the fact that even under the modified conditions, base separation is observed. It is expected that with more carefully controlled temperature boundary conditions, base separation may be further reduced or even eliminated; this is being done in ongoing work.

It is also noted that the modified cooling conditions increase the solidification time, as seen from Figure 13. It takes 2.25 hours for the casting to reach total solidification under the original con-

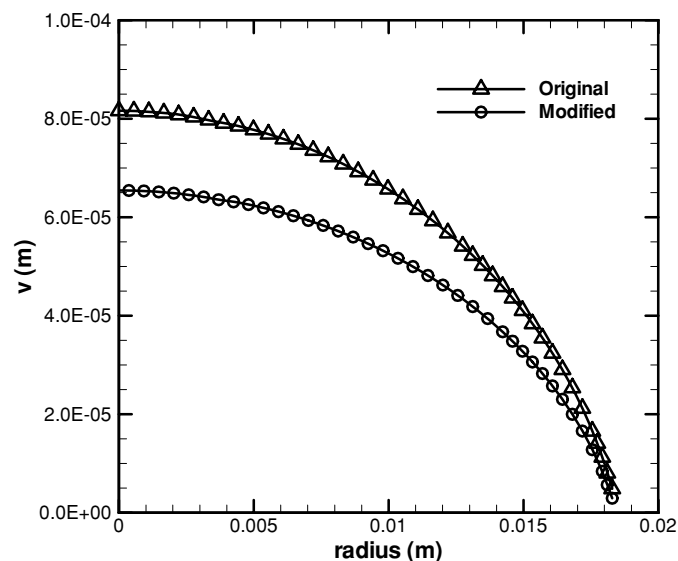


Figure 12 Comparison of vertical displacement along the bottom surface under different cooling conditions.

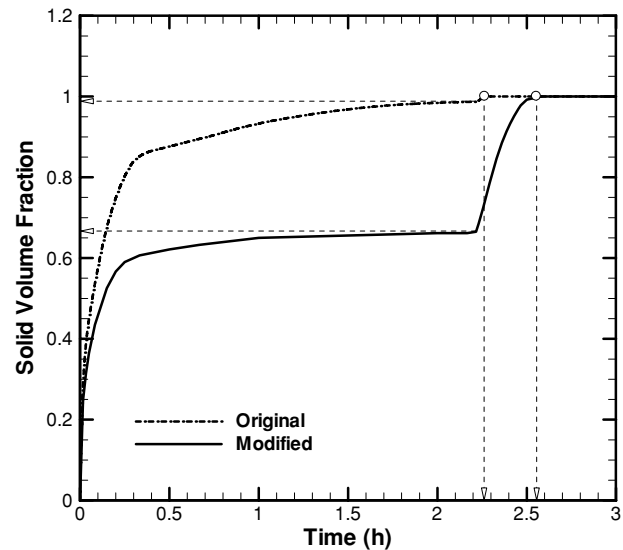


Figure 13 Solid volume fraction comparison for experimental and modified conditions.

ditions, while 2.55 hours are required using the modified condition. More of the material is held above the melting temperature during the first 2 hours under the modified conditions, leading to a solidification time that is longer by approximately 0.3 hours.

CONCLUSIONS

A comprehensive numerical investigation was conducted of the influence of cooling conditions on base separation, void formation, and thermally induced stresses during the solidification of a high Prandtl number melt in a cylindrical enclosure. A dynamically coupled model was developed to compute the heat and mass transfer processes in melt casting as well as thermal stresses induced during solidification. Improved cooling conditions were suggested based on the predicted results obtained under the experimental conditions, which were found to suppress the extent of based separation by 25%.

Ongoing enhancements to the coupled model developed in this work include an explicit consideration of mold-material separation as well as heat transfer through the gap. The particle-laden energetic material melt will also be treated as a visco-elastic-plastic material in future work.

ACKNOWLEDGMENT

The authors acknowledge financial support from the U.S. Army for this work. The project monitor was Mr. Sanjeev Singh. Neelam Naik helped with energetic material property measurements.

NOMENCLATURE

A_{mush}	mushy zone constant
b	body force

c_p	specific heat, J/kg-K
E	Young's modulus, Pa
g	acceleration due to gravity, m/s ²
G	shear modulus, Pa
h	specific enthalpy, J/kg
H_0	height of the tube and riser in cylinder casting
ΔH	latent heat, kJ/kg
k	thermal conductivity, W/m-K
p	pressure, Pa
Pr	Prandtl number, $Pr = \nu/\alpha$
R	thermal resistance
Ra	Rayleigh number, $Ra = g\beta\Delta T r^3/(\nu\alpha)$
Re	Reynolds number, $Re = UD/\nu = 1/Pr$
t	time, s
T	temperature, K
\vec{u}	velocity, m/s
\vec{w}	displacement vector, m

Greek Symbols

α	thermal diffusivity, m ² /s
β	volume expansion coefficient, 1/K
ε	solid/liquid interface thickness, discretization, m
ϕ	particle volume fraction
φ	deviation
λ	Lame's coefficient
μ	Lame's coefficient, dynamic viscosity
ν	Poisson's ratio, kinematic viscosity
ρ	density, kg/m ³
σ	stress, Pa
σ_o	yield stress, Pa
σ_R	Stefan-Boltzmann constant, 5.67×10^{-8} W/m ² -K ⁴

Subscripts

eff	effective
f	fluid
i	Cartesian component, inner, initial
l	liquid
m	melting, mold
o	outer
p	particle
s	solid
w	wall, water
∞	ambient

REFERENCES

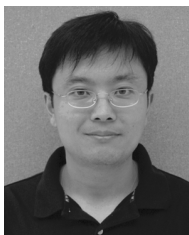
- [1] Barral, P., and Quintela, P., A Numerical Method for Simulation of Thermal Stresses during Casting of Aluminum Slabs, *Computer Methods in Applied Mechanical Engineering*, vol. 178, pp. 69–88, 1999.
- [2] Yao, L. S., and Prusa, J., Melting and Freezing, *Advances in Heat Transfer*, vol. 19, pp. 1–95, 1989.
- [3] Bertrand, O., Binet, B., Combeau, H., Couturier, S., Delannoy, Y., and Gobin, D., Melting Driven by Natural Convection, A Comparison Exercise: First Results, *International Journal of Thermal Sciences*, vol. 38, pp. 5–26, 1999.
- [4] Sun, D., Garimella, S. V., Singh, S., and Naik, N., Numerical and Experimental Investigation of the Melt Casting of Explosives, *IMECE2004-59338*, Anaheim, Calif., 2004.
- [5] Li, C. Y., Garimella, S. V., and Simpson, J. E., A Fixed-Grid Front-Tracking Algorithm for Solidification Problems, Part II—Directional Solidification with Melt Convection, *Numerical Heat Transfer B*, vol. 43, pp. 143–166, 2003.
- [6] Simpson, J. E., and Garimella, S. V., An Investigation of the Solutal, Thermal and Flow Fields in Unidirectional Alloy Solidification, *International Journal of Heat and Mass Transfer*, vol. 41, pp. 2485–2502, 1998.
- [7] Hattel, J. H., and Hansen, P. N., A 1-D Analytical Model for the Thermally Induced Stresses in the Mold Surface during Die Casting, *Applied Mathematical Modeling*, vol. 18, pp. 550–559, 1994.
- [8] Lee, M., Xiao, Y., Wittmer, D. E., Graber, T. J., and Mini, S. M., Residual Stresses in Particle-Reinforced Ceramic Composites Using Synchrotron Radiation, *Journal of Materials Science*, vol. 37, pp. 4437–4443, 2002.
- [9] Wang, X. L., Hubbard, C. R., Spooner, S., David, S. A., Rabin, B. H., and Williamson, R. L., Mapping of the Residual Stress Distribution in a Brazed Zirconia-Iron Joint, *Materials Science & Engineering A*, vol. A211, pp. 45–53, 1996.
- [10] Thomas, B. G., Issues in Thermal-Mechanical Modelling of Casting Processes, *ISIJ International*, vol. 35, pp. 737–743, 1995.
- [11] Fackeldey, M., Ludwig, A., and Sahm, P. R., Coupled Modeling of the Solidification Process Predicting Temperatures, Stresses and Microstructures, *Computational Materials Science*, vol. 7, pp. 194–199, 1996.
- [12] Seetharamu, K. N., Paragasam, R., Quadir, G. A., Zainal, Z. A., Prasad, B. S., and Sundararajan, T., Finite Element Modelling of Solidification Phenomena, *Sadhana—Academy Proceedings in Engineering Sciences*, vol. 26, pp. 103–120, 2001.
- [13] Isaac, J., Reddy, G. P., and Sharma, G. K., Numerical Prediction of Air Gap during Solidification of Casting in Metallic Moulds, *Journal of the Institution of Engineers (India)*, Part MM, vol. 69, pp. 17–22, 1988.
- [14] Taheri, F., and Murphy, J. G., Determination of Residual Stresses in Sintered Ceramics: A Hypoelastic Model, *Powder Metallurgy International*, vol. 23, pp. 101–104, 1991.
- [15] Fjaer, H., and Jensen, E. K., Mathematical Modeling of Butt Curl Deformation of Sheet Ingots—Comparison between Experimental Results for Different Starter Block Shapes, *Light Materials*, TMS, pp. 951–959, 1995.
- [16] Hannart, B., Cialti, F., and von Schalkwijk, R., Thermal Stresses in DC Casting of Aluminum Slabs: Application of a Finite Element Model, *Light Metals TMS*, pp. 879–887, 1994.
- [17] Weiner, J. H., and Boley, B. A., Elasto-Plastic Thermal Stresses in a Solidifying Body, *Journal of the Mechanics and Physics of Solids*, vol. 11, pp. 145–154, 1963.
- [18] Inoue, T., and Wang, Z. G., Thermal and Mechanical Fields in Continuous Casting Slab—A Steady State Analysis Incorporating Solidification, *Archive of Applied Mechanics (Ingenieur Archiv)*, vol. 58, pp. 265–275, 1988.

- [19] Li, C., and Thomas, B. G., Thermomechanical Finite-Element Model of Shell Behavior in Continuous Casting of Steel, *Metalurgical and Materials Transactions B*, vol. 35B, pp. 1151–1172, 2004.
- [20] Hattel, J., Hansen, P. N., and Hansen, L. F., Analysis of Thermal Induced Stresses in Die Casting Using a Novel Control Volume FDM-Technique, *Modeling of Casting, Welding and Advanced Solidification Processes*, pp. 585–592, 1993.
- [21] Liu, B. C., Kang, J. W., and Xiong, S. M., A Study on the Numerical Simulation of Thermal Stress during the Solidification of Shaped Castings, *Science and Technology of Advanced Materials*, vol. 2, pp. 157–164, 2001.
- [22] Cruchaga, M. A., Diego, J. C., and Roland, W. L., Modeling Fluid-Solid Thermomechanical Interactions in Casting Processes, *International Journal of Numerical Methods for Heat & Fluid Flow*, vol. 14, pp. 167–186, 2004.
- [23] Sun, D., Garimella, S. V., Singh, S., and Naik, N., Numerical and Experimental Investigation of the Melt Casting of Explosives, Propellants, *Explosives and Pyrotechnics*, vol. 30, no. 5, pp. 369–380, 2005.
- [24] FLUENT User Manual, Fluent Inc., 2003.
- [25] ANSYS User Manual, Ansys, 2004.
- [26] Annapragada, S. R., Sun, D., and Garimella, S. V., Prediction of Effective Thermo-Mechanical Properties of Particulate Materials, *Computational Material Science*, doi:10.1016/j.commatsci.2006.12.008, 2007.
- [27] Incropera, F. P., and DeWitt, D. P., *Fundamentals of Heat and Mass Transfer*, 4th ed., John Wiley and Sons, New York, 1996.
- [28] Beer, F. P., and Johnston, Jr., E. R., *Mechanics of Materials*, 2nd ed., McGraw-Hill, New York, 1992.
- [29] Voller, V. R., and Swaminathan, C. R., Generalized source-based method for solidification phase change, *Numerical Heat Transfer B*, vol. 19, pp. 175–189, 1991.
- [30] Carslaw, H. S., and Jaeger, J. C., *Conduction of Heat in Solids*, 2nd ed., Clarendon Press, 1959.



S. Ravi Annapragada is a Ph.D. student in the School of Mechanical Engineering at Purdue University. He worked on thermal stresses during solidification, thermo-mechanical property prediction of particulate composites, and experimental characterization of slurry solidification for his master's thesis, and received his M.S. in 2006. He obtained his bachelor's degree in 2004 from the Indian Institute of Technology, Madras, where he investigated the performance enhancement of radial fin heat exchangers. His doctoral research is focused on the material point method.

radial fin heat exchangers. His doctoral research is focused on the material point method.



Dawei Sun is a senior research engineer at Saint-Gobain High Performance Materials at Northborough, Massachusetts, USA. Prior to joining Saint-Gobain, he worked at Purdue University as a post-doctoral research associate. He received his Ph.D. in mechanical engineering from Stony Brook University in 2003. He studied at Xian Jiaotong University, China, where he obtained his B.E. and M.S. degrees. His research interests include scientific computing, materials

processing, crystal growth techniques, thermal sprays, energetic materials, property prediction of composites and multiphysics, and multiphase phenomena in phase change processes. Dr. Sun has co-authored 31 papers in archival journals and conference proceedings. He is currently working on multiphysics and multi-scale analysis of solidification processes of slurries.



Suresh V. Garimella is the R. Eugene and Susie E. Goodson Professor of Mechanical Engineering at Purdue University. He received his Ph.D. from the University of California at Berkeley in 1989. He is the director of the NSF Cooling Technologies Research Center, the Electronics Cooling Laboratory, and the Solidification Heat Transfer Laboratory. His research interests include thermal microsystems, high-performance compact cooling technologies, electro-thermal co-design and

electronics packaging, micro- and nano-scale thermal phenomena, and materials processing. Dr. Garimella has co-authored more than 225 refereed journal and conference publications, besides editing or contributing to a number of books. He serves on the editorial boards of *ASME Journal of Heat Transfer*, *Experimental Heat Transfer*, and *Experimental Thermal and Fluid Science*, and has served as editor of *Heat Transfer-Recent Contents*. He is a fellow of the ASME. His efforts in research and engineering education have been recognized with the 2004 ASME Gustus L. Larson Memorial Award, the 2006 ASME K-16 Clock Award, the Graduate School/UWM Foundation Research Award in recognition of Outstanding Research and Creative Activity (1995), the UWM Distinguished Teaching Award in recognition of Demonstrated Dedication to Excellence in Undergraduate Instruction (1997), and the Society of Automotive Engineers' Ralph R. Teetor Educational Award (1992).